Bio-green synthesis of calcium acetate from oyster shell waste at low cost and reducing the emission of greenhouse gases

Somkiat Seesanong[1], Chaowared Seangarun[2], Banjong Boonchom[2,3,4*] [ID], Nongnuch Laohavisuti[5], Somphob Thompho[6], Wimonmat Boonmee[7], Sorakit Mongkol[4] and Pesak Rungrojchaipon[4*]

Abstract

Biological wastes obtained from food, oyster shells, were recycled to calcium carbonate and then used as bio-green raw material to replace limestone/carbonate stone for calcium acetate ($Ca(CH_3COO)_2 \cdot H_2O$) production. The conditions (ambient temperature occurred in an exothermic reaction, drying time, yield, and solubility) of the reaction between the bio-green $CaCO_3$ and three different acetic (CH_3COOH) concentrations (8, 10, and 12 M) were investigated. The product's maximum yield (93%) with a shorter drying time (18 h) was obtained from the reaction between the bio-green $CaCO_3$ with 12 M acetic acid revealing a lower cost. The chemical compositions without any toxic metal impurity revealed by the X-ray fluorescence technique would be useful to suggest use in the specific application. The X-ray diffraction, Fourier Transform Infrared, and Thermogravimetric analysis data of $Ca(CH_3COO)_2 \cdot H_2O$ prepared by the bio-green $CaCO_3$ obtained from oyster shell wastes in this work and those in previous works used other calcium sources were consistent. The morphologies with different sizes of the obtained $Ca(CH_3COO)_2 \cdot H_2O$ depend on the CH_3COOH concentrations reported in this work and were different from those reported in previous works because of different calcium sources. According to the observation, it can be concluded that the low-cost and bio-green technique without the environmental effects was successfully applied to produce cheap $Ca(CH_3COO)_2 \cdot H_2O$ and reduce greenhouse gas emissions, which can be used in the specific industry.

Keywords Calcium acetate, Oyster-shell waste, Calcium carbonate, Biowaste, Thermal decomposition

*Correspondence:
Banjong Boonchom
banjong.bo@kmitl.ac.th
Pesak Rungrojchaipon
pesak.ru@kmitl.ac.th
[1] Office of Administrative Interdisciplinary Program On Agricultural Technology, King Mongkut's Institute of Technology Ladkrabang, Bangkok 10520, Thailand
[2] Material Science for Environmental Sustainability Research Unit, King Mongkut's Institute of Technology Ladkrabang, Bangkok 10520, Thailand
[3] Municipal Waste and Wastewater Management Learning Center, King Mongkut's Institute of Technology Ladkrabang, Bangkok 10520, Thailand
[4] Department of Chemistry, King Mongkut's Institute of Technology Ladkrabang, Bangkok 10520, Thailand
[5] Department of Animal Production Technology and Fishery, King Mongkut's Institute of Technology Ladkrabang, Bangkok 10520, Thailand
[6] Pharmaceutical Research Instrument Center, Chulalongkorn University, Pathumwan, Bangkok 10330, Thailand
[7] Department of Biology, King Mongkut's Institute of Technology Ladkrabang, Bangkok 10520, Thailand

1 Introduction

Commercial oysters belong to the family and principally to the genera *Ostrea* and *Crassostrea* [1]. The dominant aquaculture oyster is the Pacific (cupped) oyster, *Crassostrea gigas*, providing the greatest quantity of aquaculture species [1]. This species accounted for 97% of all oyster aquaculture production. Other aquaculture species are *Crassostrea virginica*, *Crassostrea iredalei*, *Ostrea edulis*, and *Saccostrea glomerata*. China, Japan, Korea, France, and the USA are the major oyster producers. Oyster is best known as live seafood, and most production is live, in-shell, or fresh chilled in half-shell [1]. Oyster, commonly consumed in both cooked and raw forms, is an excellent source of vitamin B_{12}, vitamin A, selenium, calcium, iron, and zinc. Other value-added products such as smoked oysters and pre-cooked meals are becoming a tradition. Two oysters (28 g) provide the Reference Daily Intake of zinc and vitamin B_{12} [2]. However, the eatable part of the oyster had only 10–16 wt%, causing about 84–90 wt % of oyster shell waste. Table 1 shows the number of farms, area, quantity, and value of Thailand's oyster production farms cultured from 2010 − 2021 [1]. From these data, the collected waste of oyster shells can be estimated as being over 60 kt per year.

The increases in shellfish aquaculture, processing industries, and seafood restaurants generate huge oyster-shell waste, which is normally dumped into coastal areas. Large numbers of shell wastes i.e., oyster shells, were unduly discarded, causing serious environmental problems for water, soil, and air, resulting in negative ecosystem health, especially in Thailand. Over time, microbial decomposition appeared and progressively created many greenhouse gases (CO_2, NO_x, NH_3, and H_2S) [2],

a serious problem that is of concern nowadays. Consequently, the bio-circular-green (BCG) economic model was introduced by the Ministry of Higher Education, Science, Research, and Innovation of Thailand to resolve various environmental problems [2]. The four industries, namely (*i*) agriculture and food, (*ii*) medical and wellness, (*iii*) bioenergy, biomaterial and biochemical, and (*iv*) tourism and creative economy, are focused and promoted according to the BCG model. Oyster-shell waste is one of the important problems needed to resolve, and an excellent method to resolve this issue is through recycling because the recycling technique can decrease the waste quantity and increase the valuable material, derived from the waste.
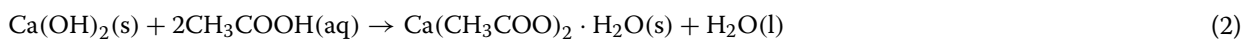
Oyster shell has a main chemical composition of 95.99% calcium carbonate ($CaCO_3$) [3]. However, other chemical compositions were also observed as oxide forms of silicon (0.70% SiO_2), magnesium (0.65% MgO), aluminum (0.42% Al_2O_3), strontium (0.33% SrO), phosphorous (0.20% P_2O_5), sodium (0.98% Na_2O), and sulfur (0.72% SO_3) [3]. Usually, $CaCO_3$ naturally occurred from two sources: non-living natural sources (limestone, carbonate rock, and ores) and living sources (eggshells and all other shells), which will have different crystal structures (calcite, aragonite, and variscite), % purity, and impurity. The $CaCO_3$ obtained from non-living natural resources has limited reserves and non-renewability. Additionally, the production process of $CaCO_3$ powder reported the CO_2 emission by IPCC.2006 found about 0.0366 kg CO_2eq kg^{-1} [4]. The oyster shells-transferred $CaCO_3$ powders obtained from living sources happened every day with collected huge amounts, which have non-limited reserves and renewability. The use of calcium carbonate from living sources as a substitute for non-living sources will help environmental problems, namely the disposal of eggshell waste/shells and the reduction of this material from calcium mineral resources, resulting in a positive effect on reducing greenhouse gas emissions [4]. So far, the $CaCO_3$ powder transformed from oyster shells has been used in various industries. For instance, it has been used in the plastic industries [5]. It is an essential ingredient in paper, paints and coatings, rubbers, adhesives, and sealants [6, 7]. It is added to plastics to reduce the cost of production. Moreover, the thermal, mechanical, and rheological properties of the resulting plastics are also improved. Due to the low cost and abundance of $CaCO_3$, it has become one of the most popular fillers for plastics. It was also used as limestone substitutes for concrete aggregates and backfills [6], as sand mixtures, cement mortars, and clinkers [7], as a calcium-enriched supplement and antimicrobial substance in the medical and pharmaceutical industries [8], as a conditioner to improve the soil quality [9], and as a calcium-mineral

Table 1 Number of farms, area, quantity, and value of Thailand's oyster production farms cultured in 2010 − 2021 [3]

Year	Number of farms	Area (km²)	Quantity (kt)	Value (Million USD)
2010	1,355	7.71	10.76	4.45
2011	997	3.71	8.38	5.95
2012	1,643	10.27	16.13	13.11
2013	1,314	7.62	17.60	13.96
2014	1,220	6.77	12.84	10.49
2015	1,208	6.80	19.87	23.10
2016	1,130	6.49	14.41	15.82
2017	985	7.19	21.92	29.72
2018	588	4.11	10.34	12.72
2019	786	9.66	17.90	22.48
2020	836	11.20	15.75	12.57
2021	1,115	9.79	13.32	8.40

Seesanong *et al. Sustainable Environment Research*   (2023) 33:26

Page 3 of 11

source for rats [8, 10]. Additionally, oyster shell powder was used as a raw agent to prepare valuable compounds such as triple superphosphate [11]. However, using oyster shells as the precursor to prepare other advanced compounds such as calcium citrate ($Ca_3(C_6H_5O_7)_2$), calcium lactate ($C_6H_{10}CaO_6$), calcium acetate ($Ca(CH_3COO)_2$), etc. still lacks fundamental information.

This work focuses on the generation of calcium acetate ($Ca(CH_3COO)_2$) from shell waste; it is known as lime acetate and vinegar salts, and the monohydrate ($Ca(CH_3COO)_2 \cdot H_2O$) form is the most common form of calcium acetate [12]. However, another form of calcium acetate, i.e., hemihydrate form, was also synthesized by Abrahams et al. [13] and Bette et al. [14]. Bette et al. [12] also reported that calcium acetate hydrate can be synthesized by the reaction between vinegar (an aqueous solution of acetic acid, CH_3COOH) and $CaCO_3$ derived from different calcium sources such as hydrated lime (calcium hydroxide, $Ca(OH)_2$), marble ($CaCO_3$), limestone ($CaCO_3$), and carbonate rocks ($CaCO_3$) according to the Eqs. (1) and (2):

$$CaCO_3(s) + 2CH_3COOH(aq) \rightarrow Ca(CH_3COO)_2 \cdot H_2O(s) + CO_2(g) \qquad (1)$$

$$Ca(OH)_2(s) + 2CH_3COOH(aq) \rightarrow Ca(CH_3COO)_2 \cdot H_2O(s) + H_2O(l) \qquad (2)$$

Calcium acetate was also synthesized by using the littleneck clam [15], black snail [16], scallop shell [17], and eggshells [18], as the starting materials. The results observed from the previous works exhibited that the physicochemical characteristics of calcium acetate depended on the starting materials and the operating conditions used in the calcium acetate preparation.

Calcium acetate was used as a promising chemical for environmental and industrial applications [14–18]. In the environmental field, it was employed as an alternative compound to replace corrosive deicers with environmentally unacceptable properties such as calcium chloride and sodium chloride [19]. It was employed as the adsorbent to absorb the carbon dioxide (CO_2) gas, which positively results in to decrease in the greenhouse effect [20]. In food processing, calcium acetate (under the number E263) was used as the coagulant in the manufacture of tofu, as a stabilizer in food and syrups, as an anti-roping agent in bread, as a stabilizer in hard candies, and as a stabilizer and preservative in many food substances [21]. It was employed to precipitate milk fat globule membrane proteins from dairy by-products [22]. For other applications, calcium acetate was employed as the precursor to synthesize various advanced materials such as nano CaO [23], cement mortar [6, 7], calcium sulfate [24], ceramic

composites [14], acetone [25], and calcium phosphate [11]. It was employed to determine the potential acidity of tropical soils and to alleviate yield loss in rice [26]. It was employed as a soil amendment, as a plant micronutrient, as foliar fertilizer, and as a soil pH adjuster [9, 17]. In addition, it was employed to treat or prevent calcium deficiency and hyperphosphatemia in patients [8].

The synthesis of calcium acetate is important for various industrial applications. In addition, the synthesis of calcium acetate from the waste can reduce the amount of waste, also increase the value of that waste, reduce the use of this raw material from ores, and reduce the emission of greenhouse gases, which is in line with the BCG strategies in Thailand [2, 4]. Consequently, this work focused on the use of oyster shells to transform $CaCO_3$ powder and then reacted with the CH_3COOH to synthesize the calcium acetate. This research presented an effective technique to generate calcium acetate by using renewable resources instead of those non-renewable resources. This designed synthesis method also helps to avoid various adverse environmental effects. The effects of the operating parameters in the calcium acetate synthesis processes such as the CH_3COOH concentration were investigated. All studied parameters were carried out to achieve the optimized conditions used to prepare calcium acetate. The physicochemical properties of the synthesized calcium acetate (yield and solubility), its characteristics (X-ray fluorescence (XRF), infrared adsorption, X-ray diffraction (XRD), thermal decomposition, and morphology) as well as the production cost were also investigated and discussed.

2 Experiment

2.1 Materials and reagents

The oyster shell wastes were collected from the Sai Kaew (12.74210, 100.84089) and Bang Saen (13.28355, 100.91514) beaches, Chonburi province, Thailand. The oyster shell wastes were first rinsed with distilled water to remove dust and various impurities and then dried in sunlight for 3 h. The clean-dried oyster shells were ground and sieved using U.S. mesh number 50 (0.297 mm) (Figure S1). The obtained powder was characterized by XRF technique and found to contain 95.25% $CaCO_3$, which was used as a starting reagent replacing minerals (limestone and carbonate rock). Additionally, the non-uniform polyhedral shapes with particle size

Seesanong *et al. Sustainable Environment Research*   (2023) 33:26

Page 4 of 11

distributions in the range of 1–6 μm were revealed by scanning electron microscope (SEM) technique (supplementary information). The $CaCO_3$ powder obtained from oyster shells was referred to as bio-green calcium carbonate. Commercial concentrated acetic acid (99.7 wt% CH_3COOH, industrial grade, Merck) was used as one of the starting reagents to synthesize the calcium acetate. CH_3COOH was used without further purification and its molarity was 17.42 M. Before use, this concentrated acid was first diluted with deionized water to prepare three different concentrations of CH_3COOH, namely 8, 10, and 12 M. Because the dilution processes were strong exothermic processes, the dilution solutions were therefore left to cool before further use.

2.2 Calcium acetate preparation

Calcium acetate monohydrate was prepared according to Eq. (1) and an example preparation was described in detail. Firstly, 8 M CH_3COOH (50 mL, 0.40 mol) was added into a beaker containing 21.02 g (0.20 mol) of the bio-green $CaCO_3$ (molecular weight of $CaCO_3$: 100.09 $g \cdot mol^{-1}$). The mixture reaction was stirred at 200 rpm for 30 min under an exothermic process occurring the released carbon dioxide (CO_2) gas. After that, the mixture reaction was exposed to the air atmosphere at ambient conditions (room temperature and 101 kPa) until it was completely dried, resulting in the formation of the pale cream-white $Ca(CH_3COO)_2 \cdot H_2O$ powder. The $Ca(CH_3COO)_2 \cdot H_2O$ powder synthesized by the reaction of 8 M CH_3COOH was designated as CA8. For the other two products, the preparation processes were similar way but different CH_3COOH concentrations of 10 and 12 M were used, and the resulting products were respectively designated as CA10 and CA12. The conditions of synthesis along with the yield, drying time, and ambient temperature were followed and recorded. The optimum parameters will be discussed.

2.3 Characterization

After three $Ca(CH_3COO)_2 \cdot H_2O$ samples (CA8, CA10, and CA12) were synthesized from the reaction between bio-green $CaCO_3$ and different CH_3COOH concentrations, a synchrotron rapid-scanning XRF (model 3400, Bruker) spectrophotometer was used to analyze the elemental composition and amount of trace elements in the synthesized samples. The structure and crystallinity of samples were investigated by D8 Advance XRD (Bruker) with Cu-Kα X-ray source (wavelength, λ, of 1.5406 Å). The 2θ values were scanned and collected from 5 to 60 degrees (°) with 0.01° scan step. To investigate and confirm the synthesized materials, the resulting diffraction patterns were compared and matched with the Joint Committee on Powder Diffraction Standards (JCPDS) card number (#), a crystallographic database [12–14]. The vibrational characteristics (chemical bonds of the molecular structures) of the synthesized compounds were recorded and analyzed by the Spectrum GX Fourier transform infrared (FTIR) spectrophotometer (Perkin Elmer) using the potassium bromide (KBr) disk technique [18]. The wavenumber ranged from 4000 to 400 cm^{-1} with a resolution of 2 cm^{-1} [17]. To prepare the FTIR sample, the synthesized $Ca(CH_3COO)_2 \cdot H_2O$ was homogeneously mixed with the spectroscopic-grade KBr powder using an agate mortar. Obtained finely ground was hydraulically compressed into a pellet, which was then put into a sample holder of the spectrophotometer. The Pyris Diamond thermogravimetric/differential thermal analyzer (TGA/DTA, Perkin Elmer) was used to perform the thermogravimetric (TG) and differential thermogravimetric (DTG) measurements in the N_2 atmosphere from ambient temperature (30 °C) to 900 °C at a heating rate of 5 $°C \cdot min^{-1}$. Finally, the surface morphologies of the synthesized samples and raw materials (Figure S1) were observed with a SEM (LEO 1450 VP) by applying a gold-coated technique before analysis [17].

3 Results and discussion

3.1 Preparation optimization results

Three $Ca(CH_3COO)_2 \cdot H_2O$ samples (CA8, CA10, and CA12) were successfully prepared from the reaction between bio-green $CaCO_3$ and three different CH_3COOH concentrations (8, 10, and 12 M). Four conditions based on the synthesis of $Ca(CH_3COO)_2 \cdot H_2O$ by using bio-green $CaCO_3$ and CH_3COOH are ambient temperature that occurred in an exothermic reaction, drying time, yield, and solubility. The advantages of $Ca(CH_3COO)_2 \cdot H_2O$ production from the bio-green $CaCO_3$ obtained from oyster shell waste precursor are able to achieve a high yield with a short drying time. These conditions point out the low production cost, which can affect the economic decision of the users.

Table 2 shows the ambient temperatures that occurred in an exothermic reaction, drying times, yields, and solubilities obtained from the $Ca(CH_3COO)_2 \cdot H_2O$ production using different CH_3COOH concentrations. Obviously, the yields of more than 89% of all $Ca(CH_3COO)_2 \cdot H_2O$ samples from each acid concentration were observed, and the maximum yield of 93% was obtained from using 10 or 12 M CH_3COOH. The yields of the $Ca(CH_3COO)_2 \cdot H_2O$ production obtained from oyster shells reported in this work are higher than those prepared from scallop shells reported in our previous work (87%) [17]. The temperature due to the exothermic reaction of the $Ca(CH_3COO)_2 \cdot H_2O$ synthesis was

Table 2 The parameters of the $Ca(CH_3COO)_2 \cdot H_2O$ production from the reaction between the different CH_3COOH concentrations and bio-green $CaCO_3$

Sample codes	[CH_3COOH] (M)	Ambient temperature occurred in reaction (°C)	Drying time (h)	Yields (%)	Solubilities (%)
CA8	8	37	30	89	97.6
CA10	10	42	24	93	97.3
CA12	12	58	18	93	96.6

observed in the range of $37-58$ °C, which increased with increasing CH_3COOH concentration. The temperature of $Ca(CH_3COO)_2 \cdot H_2O$ production in this work is slightly different from those of the $Ca(CH_3COO)_2 \cdot H_2O$ synthesized by scallop shells in our previous work (35–64 °C) [17]. The drying time, recorded at the beginning of the reaction until the powder completely dried by itself was observed in 18–30 h, which decreased with increasing CH_3COOH concentration. The drying time of the $Ca(CH_3COO)_2 \cdot H_2O$ production obtained from oyster shells in this work is a longer time than those of scallop shells in our previous work (10–24 h) [17]. The solubilities of all $Ca(CH_3COO)_2 \cdot H_2O$ samples are nearly the same value of 97%. The conditions of $Ca(CH_3COO)_2 \cdot H_2O$ production are caused by different calcium sources (oyster shells and scallop shells), related to the purities of calcium carbonate [17].

The optimal condition for the $Ca(CH_3COO)_2 \cdot H_2O$ production with short drying time and higher yields were found in the reaction between the bio-green $CaCO_3$ and 12 M CH_3COOH. The obtained conditions can be applied to an industrial scale to obtain the highest $Ca(CH_3COO)_2 \cdot H_2O$ yield. This $Ca(CH_3COO)_2 \cdot H_2O$ synthesis technique using shell waste is attractive economically and environmentally. The cost of the bio-green $CaCO_3$ (95.3% purity) powders obtained from oyster shells determined by costs of transportation, plant, labor, water, and electricity was estimated at about 0.033 $USD \cdot kg^{-1}$. The cost of CH_3COOH (industrial grade, density of 1.049 $g \cdot mL^{-1}$) used in this work is about 0.6 $USD \cdot kg^{-1}$ or 0.625 $USD \cdot L^{-1}$. In the reaction of $Ca(CH_3COO)_2 \cdot H_2O$ preparation (Eq. 1), 1.05 kg of the bio-green $CaCO_3$ (0.034 USD) required 1.14 L (1.2 kg) of CH_3COOH (0.72 USD). The yield of about 93% for the optimum condition would be about 1.64 kg of $Ca(CH_3COO)_2 \cdot H_2O$ synthesized (0.75 $USD \cdot kg^{-1}$). The overall cost of $Ca(CH_3COO)_2 \cdot H_2O$ with plant, labor, water, and electricity was estimated at about 0.030 $USD \cdot kg^{-1}$. Consequently, the cost for $Ca(CH_3COO)_2 \cdot H_2O$ product reported in this work

is about 0.78 $USD \cdot kg^{-1}$. The bulk market price of $Ca(CH_3COO)_2 \cdot H_2O$ is about 1 $USD \cdot kg^{-1}$ so producing this compound from oyster shells would be economically profitable. For environmental issues, oyster shells are wastes from food, which are usually deposited in landfills. This food waste management will be the emissions of greenhouse gases (CO_2), which were reported to be about 2.53 kg CO_2eq kg^{-1}. From Thailand, oyster shell wastes have been reported to be more than 10 kt per year, so the emissions of CO_2 are estimated more than 20 kt per year (Table S1). Additionally, calcium carbonate, raw material used for $Ca(CH_3COO)_2 \cdot H_2O$ production at plants was normally obtained from ore sources (limestone or/and carbonate stone), in which the emission factor was about 1.067 kg CO_2eq kg^{-1}. The emissions of CO_2 of the bio-green $CaCO_3$ obtained from oyster shells determined with the used process (transportation, water, and electricity) was estimated to be 0.017 kg CO_2eq kg^{-1} (Figure S2). Therefore, the emissions of CO_2 of $Ca(CH_3COO)_2 \cdot H_2O$ production calculated according to Eq. (1) are found to be 2.62 and 2.22 (2.17–2.27) kg CO_2 eq kg^{-1} for calcium carbonate obtained from ore source and oyster shell, respectively (Emission factor of acetic acid = 2.57 kg CO_2eq kg^{-1}. This result indicates that the using bio-green $CaCO_3$ obtained from oyster shells for $Ca(CH_3COO)_2 \cdot H_2O$ production leads to the reduced emissions of CO_2 of about 0.4 kg CO_2eq kg^{-1} (Table S2). Moreover, it also reduces the use of calcium carbonate from rock minerals with limited reserves in Thailand and reduces greenhouse gas emissions from the production process of this chemical. From the above discussion, using the bio-green $CaCO_3$ obtained from oyster shells for $Ca(CH_3COO)_2 \cdot H_2O$ production is more advantageous; low cost, recycling waste to high value compound, and reduction of greenhouse gas emissions.

3.2 XRF results

After applying the SRS 3400 XRF spectrophotometer, the XRF results of the synthesized $Ca(CH_3COO)_2 \cdot H_2O$ are shown in Table 3. Table 3 exhibited the chemical compositions of $Ca(CH_3COO)_2 \cdot H_2O$ products synthesized from different CH_3COOH concentrations (8, 10, and 12 M). The purities of all synthesized $Ca(CH_3COO)_2 \cdot H_2O$ samples (CA8, CA10, and CA12) based on the XRF results were not significantly different. Calcium oxide (CaO) is the main chemical composition of all $Ca(CH_3COO)_2 \cdot H_2O$ samples with contents of around 90%. Whereas silicon oxide (SiO_2) is the second chemical composition with contents of around 4%. However, some oxide forms of sodium (Na_2O), magnesium (MgO), sulfur (SO_3), aluminum (Al_2O_3), and iron (Fe_2O_3, ferric oxide)

Table 3 Chemical compositions of Ca(CH$_3$COO)$_2$·H$_2$O prepared from the reaction between the bio-green CaCO$_3$ and 8 (CA8), 10 (CA10), and 12 (CA12) M CH$_3$COOH

Chemical compounds	Formula	Chemical contents (%)		
		CA8	CA10	CA12
Calcium oxide	CaO	89.2	89.2	90.0
Silicon oxide	SiO$_2$	3.84	4.03	3.27
Sodium oxide	Na$_2$O	1.36	1.31	1.34
Magnesium oxide	MgO	1.05	1.00	1.06
Sulfur oxide	SO$_3$	1.02	0.97	1.02
Aluminum oxide	Al$_2$O$_3$	1.01	1.03	0.96
Ferric oxide	Fe$_2$O$_3$	0.98	0.98	0.85
Chloride	Cl	0.62	0.56	0.57
Strontium oxide	SrO	0.42	0.41	0.43
Phosphorous oxide	P$_2$O$_5$	0.19	0.18	0.21
Potassium oxide	K$_2$O	0.17	0.16	0.15
Titanium oxide	TiO$_2$	0.10	0.11	0.09
Manganese oxide	MnO	0.07	0.06	0.07
Boron	Br	0.02	0.02	0.01
Zinc oxide	ZnO	0.01	0.01	0.01
Copper oxide	CuO	–	0.01	–
Chromium oxide	Cr$_2$O$_3$	–	–	0.03
Summation		100	100	100

were observed with contents of around 1%. Other chemical compositions of less than 1% were also presented in Table 3. The essential trace elements (manganese (Mn) zinc (Zn), and copper (Cu)) in plants and animals, but not all microorganisms were observed with contents about 0.01–0.07%, which are enough when used in food and dietary supplement [8, 15, 16]. However, 0.03% of the chromium found in the CA12 sample requires caution because the amount used in food and medicine is controlled not more than 13 mg per serving [21, 22]. The accumulation of some toxic compounds in oyster shell waste may be observed, which depended on the natural source. Therefore, the elemental compositions of the synthesized compounds should be investigated. According to the XRF results obtained in this work, Ca(CH$_3$COO)$_2$·H$_2$O synthesized from oyster shell waste did not contain toxic elements such as cadmium (Cd), arsenic (As), lead (Pb), etc., pointing out the advantages of the oyster shell derived CaCO$_3$ as an alternative starting material to synthesize Ca(CH$_3$COO)$_2$·H$_2$O without toxic elements.

3.3 FTIR results

The Spectrum GX FTIR spectrophotometer was applied to investigate the vibrational spectroscopy of the synthesized Ca(CH$_3$COO)$_2$·H$_2$O (CA8, CA10, and CA12) compounds. The FTIR spectra of all samples are very
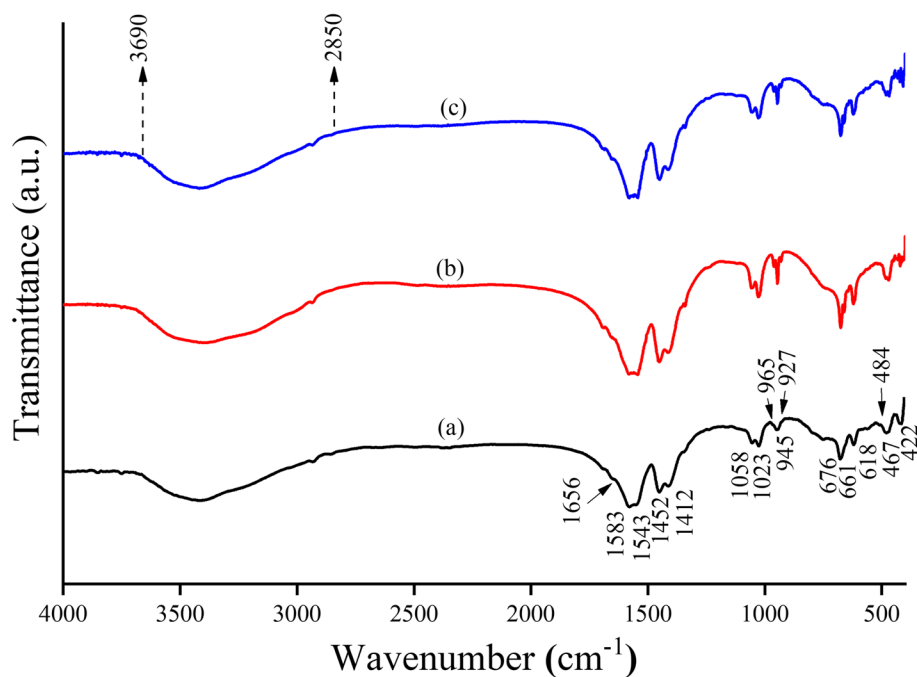
Fig. 1 Flourier transform infrared (FTIR) spectra of Ca(CH$_3$COO)$_2$·H$_2$O compounds prepared from the reaction between the bio-green CaCO$_3$ and three acetic concentrations (**a** CA8, **b** CA10 and **c** CA12)

Seesanong *et al. Sustainable Environment Research*   (2023) 33:26

Page 7 of 11

similar and are shown in Fig. 1. The vibrational broad bands in the $3690-2850$ cm^{-1} region were assigned as the symmetric $\nu_s(H_2C-H)$ and asymmetric $\nu_{as}(H_2C-H)$ vibrational stretching modes of methyl (CH_3) group as well as the symmetric $\nu_s(O-H)$ and asymmetric $\nu_{as}(O-H)$ stretching modes of water (H_2O) molecule. The weak peak at 1656 cm^{-1} contributed to the symmetric $\nu_3(H-O-H)$ bending mode of H_2O [12]. Two strong adsorption peaks at 1583 and 1543 cm^{-1} are assigned as the asymmetric $\nu_{as}(C-O)$ stretching vibrational mode, while two intense peaks at 1452 and 1412 cm^{-1} are assigned as the symmetric $\nu_s(C-O)$ stretching vibrational mode of the $C-O$ bond of the acetate anion (CH_3COO^-) [13]. The out of plane $\rho_{op}(CH_3)$ stretching vibration of CH_3 group was split into two peaks at 1058 and 1023 cm^{-1}, whereas the $\nu(C-C)$ stretching vibration of CH_3COO^- divided into three peaks at 965, 945, and 927 cm^{-1}. Three peaks at 676, 661, and 618 cm^{-1} are the out-of-plane $\rho_{op}(OCO)$ stretching vibrational modes of the $O-C-O$ group of CH_3COO^-. Finally, three weak peaks, that appeared in all spectra of $Ca(CH_3COO)_2 \cdot H_2O$ compounds at about 484, 467, and 422 cm^{-1} are assigned as the in-plane $\rho_{ip}(OCO)$ bending vibrational mode of the $O-C-O$ group of CH_3COO^- [12, 13]. These results are similar to the reported by Chung et al. [19] and Thongkam et al. [17], in a previous report of calcium acetate prepared from oyster shells and scallop shells. Therefore, the FTIR spectra of all prepared samples confirmed that the synthesized products are calcium acetate monohydrate ($Ca(CH_3COO)_2 \cdot H_2O$).

3.4 XRD results

The crystal structure of the synthesized calcium acetate compounds was characterized by the D8 Advance X-ray diffractometer. Figure 2 presented the XRD patterns of the calcium acetate samples prepared from three different CH_3COOH concentrations (8, 10, and 12 M). The XRD results were compared with those of calcium acetate reported by previous reports [12–16]. The XRD pattern clearly showed that the product synthesized from the reaction between the bio-green $CaCO_3$ and CH_3COOH is the calcium acetate monohydrate ($C_4H_6CaO_4 \cdot H_2O$ or $Ca(CH_3COO)_2 \cdot H_2O$), which was found to match with the JCPDS card #19–0200 [27]. This JCPDS number obtained in this work is different from that of $Ca(CH_3COO)_2 \cdot H_2O$ prepared from scallop shell in literature (JCPDS card #19–0200) [27]. The XRD patterns of all synthesized $Ca(CH_3COO)_2 \cdot H_2O$ products are quite similar, pointing out that the phases of all $Ca(CH_3COO)_2 \cdot H_2O$ compounds prepared from different CH_3COOH concentrations are different. Furthermore, all XRD patterns of the $Ca(CH_3COO)_2 \cdot H_2O$ compounds are in good agreement with the reference data given by Van der Sluis et al. [27] and Klop et al. [28]. The XRD results of all the prepared samples obtained are in line with the FTIR data, which confirm the identification of each $Ca(CH_3COO)_2 \cdot H_2O$ compound.

The crystal structure of $Ca(CH_3COO)_2 \cdot H_2O$ was investigated and well-described by Klop et al. [28]. $Ca(CH_3COO)_2 \cdot H_2O$ (MW = 176 g·mol^{-1}) crystallizes in a triclinic crystal system with the space group of *P1* (space group number 1), Schoenflies symbol of C_1^1. The crystal
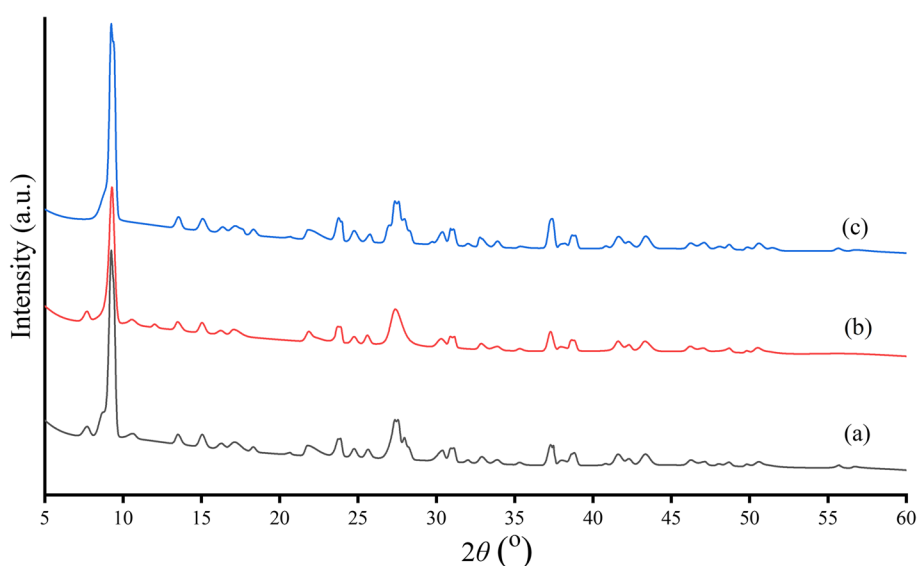
Fig. 2 X-ray diffraction (XRD) patterns of $Ca(CH_3COO)_2 \cdot H_2O$ compounds prepared from the reaction between the bio-green $CaCO_3$ and three acetic concentrations (**a** CA8, **b** CA10 and **c** CA12)

structure of $Ca(CH_3COO)_2 \cdot H_2O$ consists of infinite multiple O-bridged double-stranded Ca chains, which are cross-linked via the H bonds. The lattice parameters are $a = 6.751$ Å, $b = 11.08$ Å, and $c = 11.78$ Å with. The lattice angles are $\alpha = 116.50°$, $\beta = 92.41°$, and $\gamma = 97.32°$. The unit cell's volume and the number of molecules (or formula units) in the unit cell are 777.1 Å^3 and 4, respectively. Whereas the density value of $= 1.51$ g·cm^{-3} [28].

3.5 TGA results

After applying the Pyris Diamond thermal analyzer, the resulting TG and DTG curves of the synthesized $Ca(CH_3COO)_2 \cdot H_2O$ compounds are demonstrated in Fig. 3. The curves were measured and recorded in the temperature range from $30 - 900$ °C. It was observed that the TG curves of the $Ca(CH_3COO)_2 \cdot H_2O$ prepared from three different CH_3COOH concentrations (CA8, CA10, and CA12) (Fig. 3a–c) were similar with three thermal transformation reaction regions occurring in around $70 - 190$, $300 - 520$, and $550 - 730$ °C, with the corresponding mass-loss of around 10, 30, and 25%,

respectively for all $Ca(CH_3COO)_2 \cdot H_2O$ samples. The total mass-loss was ~65%, whereas the retained mass was ~35%. The total mass loss and the residual mass of all prepared $Ca(CH_3COO)_2 \cdot H_2O$ products were different from the values obtained from the theoretical data (about 32%) and the same compound prepared by scallop shell (34%) [17]. The higher residual mass observed in this work confirms the metal impurities (Si, Na, Mg, Al, Fe, etc.) in all obtained products, which are well consistent with XRF data. The thermal decomposition reaction of $Ca(CH_3COO)_2 \cdot H_2O$ generated calcium oxide (CaO) as the final decomposed product with stable properties, which can be applied in various industrial fields, especially biodiesel production [23].

The DTG curves of all $Ca(CH_3COO)_2 \cdot H_2O$ (CA8, CA10, and CA12) samples were quite similar, and five DTG peaks at similar temperatures ($108 - 117$, $164 - 116$, $420 - 425$, $485 - 506$, and $692 - 700$ °C) were observed. The first TG mass-loss section corresponded to the two-first DTG peaks for all synthesized $Ca(CH_3COO)_2 \cdot H_2O$ compounds. The number of the
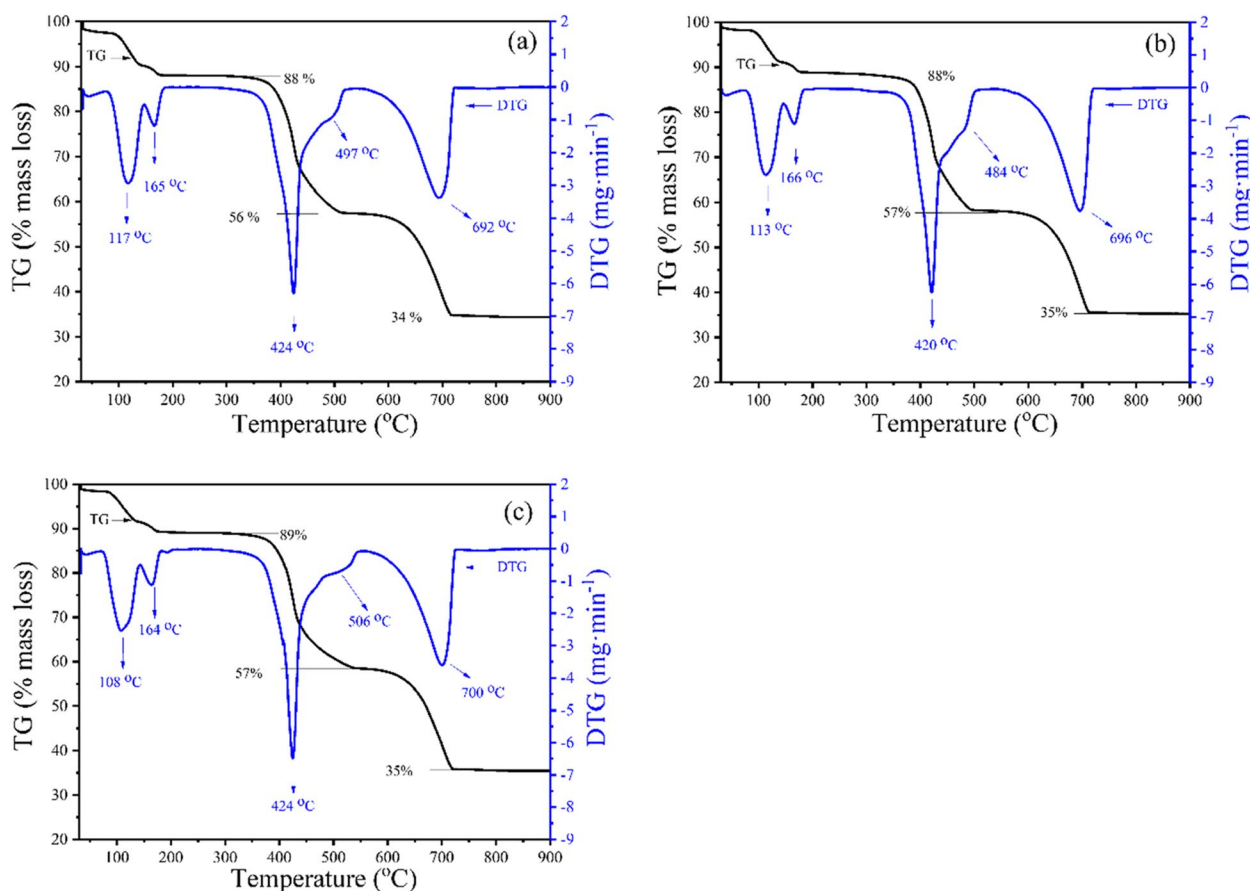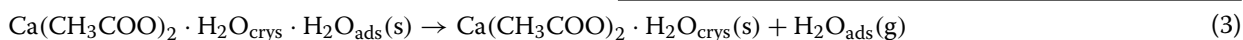

Fig. 3 Thermal analytic (TG and DTG) curves of $Ca(CH_3COO)_2 \cdot H_2O$ compounds prepared from the reaction between the bio-green $CaCO_3$ and three acetic concentrations (**a** CA8, **b** CA10 and **c** CA12)
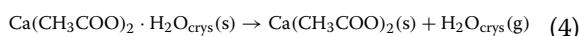
two-first DTG peaks pointed out the unlike surrounding environment of the water molecules. These two-first DTG peaks were assigned as the eliminations of adsorbed water (H_2O_{ads}, first DTG peak, $108-117$ °C) and water of the $Ca(CH_3COO)_2 \cdot H_2O$ crystal structure (H_2O_{crys}, second DTG peak, $164-116$ °C), which called "dehydration", resulting in the formation of calcium acetate anhydrous ($Ca(CH_3COO)_2$), which is a good agreement to the results reported by Bette et al. [12, 14]. The second TG mass-loss section was related to two individual peaks ($420-425$ and $485-506$ °C) that occurred in DTG curves for all synthesized $Ca(CH_3COO)_2 \cdot H_2O$ samples. The third DTG peak ($420-425$ °C) was assigned as the decomposition of $Ca(CH_3COO)_2$, resulting in the formation of $CaCO_3$ together with the elimination of acetone (CH_3COCH_3) compound (deacetonation). Whereas the fourth DTG peak ($485-506$ °C) was assigned as the decomposition of CH_3COCH_3, forming and eliminating the ketene (H_2CCO, formal name: ethenone) (deketenation) and methane (CH_4) (demethanation) [17, 25]. After that, the final TG mass-loss section with the single DTG peak ($692-700$ °C) was assigned as the decomposition of $CaCO_3$, resulting in the formation of CaO together with the elimination of CO_2 (decarbonization). From the thermal analysis (TG and DTG) results, the thermal decomposition processes of all synthesized calcium acetate samples could be written as the following equations (Eqs. (3)−(7)):
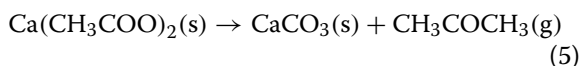
First DTG peak: Dehydration, $108-117$ °C

$$Ca(CH_3COO)_2 \cdot H_2O_{crys} \cdot H_2O_{ads}(s) \rightarrow Ca(CH_3COO)_2 \cdot H_2O_{crys}(s) + H_2O_{ads}(g) \tag{3}$$

Second DTG peak: Dehydration, $164-116$ °C

$$Ca(CH_3COO)_2 \cdot H_2O_{crys}(s) \rightarrow Ca(CH_3COO)_2(s) + H_2O_{crys}(g) \tag{4}$$

Third DTG peak: Deacetonation, $420-425$ °C

$$Ca(CH_3COO)_2(s) \rightarrow CaCO_3(s) + CH_3COCH_3(g) \tag{5}$$

Fourth DTG peak: Deketenation and demethanation, $485-506$ °C

$$CH_3COCH_3(g) \rightarrow H_2CCO(g) + CH_4(g) \tag{6}$$

Fifth DTG peak: Decarbonization, $692-700$ °C

$$CaCO_3(s) \rightarrow CaO(s) + CO_2(g) \tag{7}$$

The results of TG and DTG from this work show that the thermal decomposition of the synthesized $Ca(CH_3COO)_2 \cdot H_2O$ from oyster shells is close to the previously reported calcium acetate monohydrate ($Ca(CH_3COO)_2 \cdot H_2O$) prepared from scallop shells by Thongkam et al. [17] with the same decomposition pattern and temperature.

3.6 SEM results

After applying the LEO 1450 VP SEM, Fig. 4 illustrated the resulting SEM images of the $Ca(CH_3COO)_2 \cdot H_2O$ compounds synthesized from three different CH_3COOH concentrations (CA8, CA10, and CA12). The SEM images of three $Ca(CH_3COO)_2 \cdot H_2O$ samples as presented in Fig. 4a–c illustrated similar morphologies. The SEM results showed the aggregation of the timber-like particles with many irregular particles, especially the CA12 sample. It can be noted that the distributions of the sample particle sizes increased with increasing CH_3COOH concentration. The dimensions of the particles are in the range of $1-30$ μm. The timber-like morphology for the CA8 sample occurred more than those of other $Ca(CH_3COO)_2 \cdot H_2O$ samples. On the other hand, the irregular particle was observed when 12 M CH_3COOH was used in the $Ca(CH_3COO)_2 \cdot H_2O$ preparation. The morphologies of all $Ca(CH_3COO)_2 \cdot H_2O$ particles synthesized by bio-green $CaCO_3$ powder obtained in this work were different in both shapes and sizes from $Ca(CH_3COO)_2 \cdot H_2O$ synthesized by $CaCO_3$ powder by using the littleneck clam [15], black snail [16] and scallop [17] shells which depended on the crystal structure and particle sizes of the starting materials. These phenomena pointed out that the starting materials, used in the $Ca(CH_3COO)_2 \cdot H_2O$ synthesis, exert a significant impact on the $Ca(CH_3COO)_2 \cdot H_2O$ morphology. These results agree with the results reported by Bette et al. [12, 14].

4 Conclusions

Three $Ca(CH_3COO)_2 \cdot H_2O$ samples were successfully synthesized from the exothermic reaction between the bio-green $CaCO_3$ and various CH_3COOH concentrations. The influences of some operating parameters, i.e., the concentrations of CH_3COOH (8, 10, and 12 M), on the reaction temperature, drying time, and yield during the $Ca(CH_3COO)_2 \cdot H_2O$ formation were investigated. The optimum conditions focused on the maximum yield with the short drying time were obtained by using a high CH_3COOH concentration. XRF results confirmed that the chemical composition and purity could indicate no toxic metal in the prepared samples, which will be useful in a specific application such as fertilizer, feed minerals, food additives, etc. FTIR and TGA results of all samples in this work are similar to those from the previous report but the obtained XRD and SEM data are different.
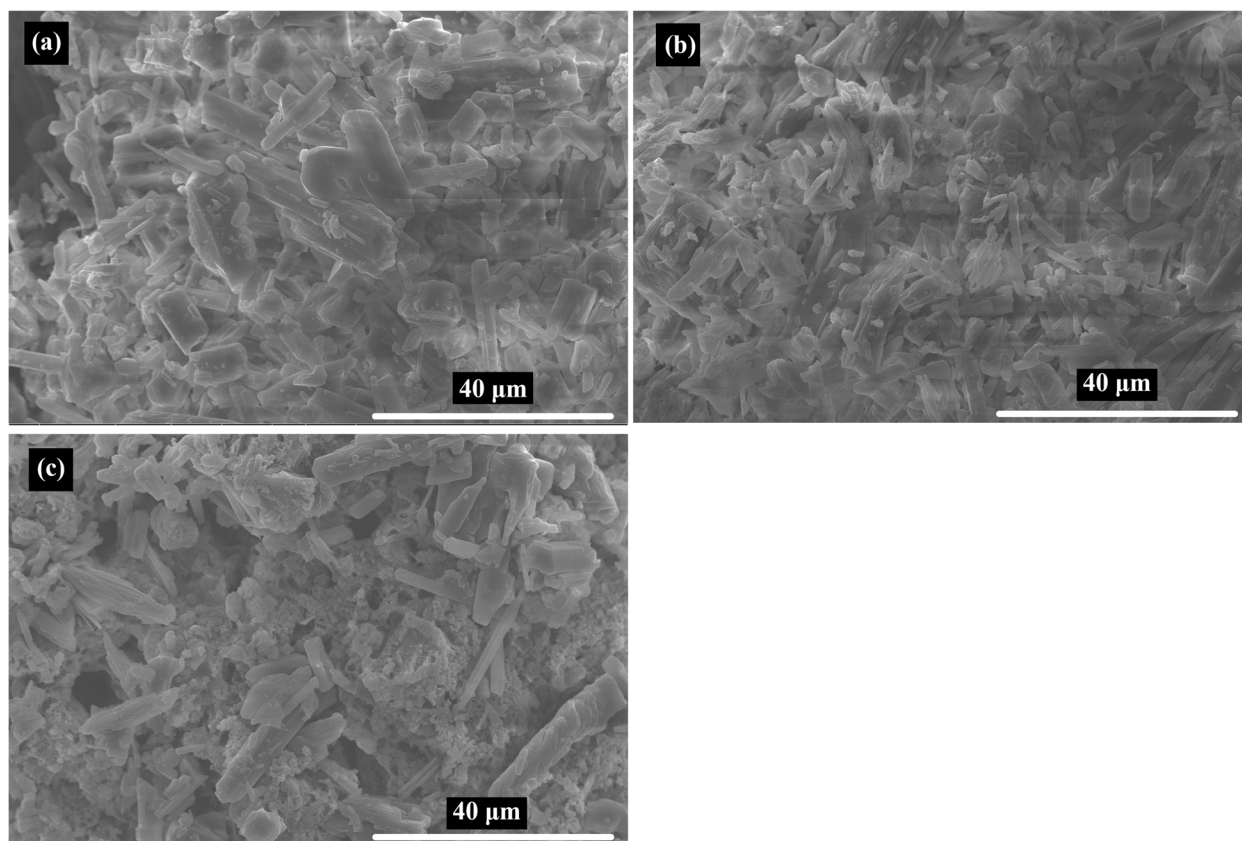
Fig. 4 Scanning electron microscopic (SEM) images of Ca(CH$_3$COO)$_2$·H$_2$O compounds prepared from the reaction between the oyster-shell derived CaCO$_3$ and 8 (**a**), 10 (**b**), and 12 (**c**) M CH$_3$COOH

This is possible because of raw materials sources with different purity. In conclusion, this research presents valuable information and an alternative method for Ca(CH$_3$COO)$_2$·H$_2$O production for various applications by using oyster shell waste as starting materials to replace the natural ores, limited reserves. Moreover, the management of oyster shell waste in this work can help reduce emissions of greenhouse gases by recycling wastes and reducing using calcium carbonate from ore sources.

Supplementary Information

The online version contains supplementary material available at https://doi.org/10.1186/s42834-023-00187-6.

Additional file 1: Table S1. Calculation of carbon emissions in the production of the bio-green CaCO$_3$ powder obtained from oyster shell wastes [1, 2]. **Table S2** Calculation of carbon emissions in the production of calcium acetate from the reaction of the bio-green CaCO$_3$ powder obtained from oyster shell wastes and various acetic acid concentrations [1, 2]. **Fig. S1.** SEM micrograph of the bio-green CaCO$_3$ powder obtained from the oyster shell. **Fig. S2.** Process line of production for the bio-green CaCO$_3$ powder obtained from oyster shell wastes [1].

Authors' contributions
Conceptualization, S.S., B.B., and P.R.; methodology, S.T., C.S., and S. M.; investigation, P.R. and C.S.; data curation, W.B., N.L., and P.R.; writing—original draft preparation, C.S., W.B., and S.S; writing—review and editing, C.S., S.S. and B.B.; visualization, W.B; supervision, S.S. and N.L.; project administration, B.B; funding acquisition, P.R. All authors read and approved the final manuscript.

Availability of data and materials
All data generated or analyzed during this study are included in this published article.

Declarations

Competing interests
The authors declare no conflict of interest. The funders had no role in the design of the study; in the collection, analyses, or interpretation of data; in the writing of the manuscript, or in the decision to publish the results.

References

1. FAO. The State of World Fisheries and Aquaculture 2022. Towards Blue Transformation. Rome: Food and Agriculture Organization of the United Nations; 2022.
2. Laohavisuti N, Boonchom B, Boonmee W, Chaiseeda K, Seesanong S. Simple recycling of biowaste eggshells to various calcium phosphates for specific industries. Sci Rep. 2021;11:15143.
3. Yoon GL, Kim BT, Kim BO, Han SH. Chemical–mechanical characteristics of crushed oyster-shell. Waste Manage. 2003;23:825–34.
4. Thailand Greenhouse Gas Management Organization. Emission Factor Categorized by Industry Group. 2022. [in Thia] http://thaicarbonlabel.tgo.or.th/admin/uploadfiles/emission/ts_af09c20f4f.pdf (Accessed 17 Jul 2023).
5. Lin Y, Chan CM. Ch 3: Calcium carbonate nanocomposites. In: Gao F, editor. Advances in Polymer Nanocomposites. Sawston: Woodhead; 2012.
6. Eziefula UG, Ezeh JC, Eziefula BI. Properties of seashell aggregate concrete: A review. Constr Build Mater. 2018;192:287–300.
7. Her S, Park T, Zalnezhad E, Bae S. Synthesis and characterization of cement clinker using recycled pulverized oyster and scallop shell as limestone substitutes. J Clean Prod. 2021;278:123987.
8. Xu Y, Ye J, Zhou D, Su L. Research progress on applications of calcium derived from marine organisms. Sci Rep-Uk. 2020;10:18425.
9. Ghimire KN, Kai H, Inoue K, Ohto K, Kawakita H, Harada H, et al. Heavy metal removal from contaminated scallop waste for feed and fertilizer application. Bioresource Technol. 2008;99:2436–41.
10. Chen N, Hu W, Feng C, Zhang Z. Removal of phosphorus from water using scallop shell synthesized ceramic biomaterials. Environ Earth Sci. 2014;71:2133–42.
11. Seesanong S, Seangarun C, Boonchom B, Sronsri C, Laohavisuti N, Chaiseeda K, et al. Recrystallization of triple superphosphate produced from oyster shell waste for agronomic performance and environmental issues. Minerals. 2022;12:254.
12. Bette S, Eggert G, Emmerling S, Etter M, Schleid T, Dinnebier RE. Crystal structure, polymorphism, and anisotropic thermal expansion of α-Ca(CH3COO)$_2$. Cryst Growth Des. 2020;20:5346–55.
13. Abrahams BF, Commons CJ, Hudson TA, Sanchez Arlt RW. The elusive crystals of calcium acetate hemihydrate: chiral rods linked by parallel hydrophilic strips. CrystEngComm. 2021;23:707–13.
14. Bette S, Stelzner J, Eggert G, Schleid T, Matveeva G, Kolb U, et al. Corrosion of heritage objects: collagen-like triple helix found in the calcium acetate hemihydrate crystal structure. Angew Chem Int Edit. 2020;59:9438–42.
15. Park SH, Jang SJ, Lee HJ, Lee GW, Lee JK, Kim YJ, et al. Optimization of calcium acetate preparation from littleneck clam (*Ruditapes philippinarum*) shell powder and its properties. Korean J Food Sci Technol. 2015;47:321–27 [In Korean].
16. Lee MY, Lee YK, Kim SD. Quality characteristics of calcium acetate prepared with vinegars and ash of black snail. J Korean Soc Food Sci Nutr. 2004;33:593–597 [In Korean]. https://doi.org/10.3746/jkfn.2004.33.3.593 (Accessed 13 Jul 2023).
17. Thongkam M, Saelim J, Boonchom B, Seesanong S, Chaiseeda K, Laohavisuti N, et al. Simple and rapid synthesis of calcium acetate from scallop shells to reduce environmental issues. Adsorpt Sci Technol. 2021;2021:6450289.
18. Nobre LCS, Santos S, Palavra AMF, Calvete MJF, de Castro CAN, Nobre BP. Supercritical antisolvent precipitation of calcium acetate from eggshells. J Supercrit Fluid. 2020;163:104862.
19. Chung KH, Jung SC, Park BG. Eco-friendly deicer prepared from waste oyster shells and its deicing properties with metal corrosion. Environ Technol. 2021;42:3360–8.
20. Uysal Ziraman D, Dogan OM, Uysal BZ. Kinetics of chemical absorption of carbon dioxide into aqueous calcium acetate solution. Int J Chem Kinet. 2020;52:251–65.
21. Lu JY, Carter E, Chung RA. Use of calcium salts for soybean curd preparation. J Food Sci. 1980;45:32–4.
22. Price N, Fei T, Clark S, Wang T. Application of zinc and calcium acetate to precipitate milk fat globule membrane components from a dairy by-product. J Dairy Sci. 2020;103:1303–14.
23. Liu X, Shi J, He L, Ma X, Xu S. Modification of CaO-based sorbents prepared from calcium acetate for CO2 capture at high temperature. Chinese J Chem Eng. 2017;25:572–80.
24. Chen S, Fu J, He X, Su Y, Xiong G, Liu Q, et al. Microemulsion synthesis of anhydrous calcium sulfate nanowhiskers with calcium acetate solution and its surface structure stable and crystal phase evolution after modification. J Nanopart Res. 2020;22:193.
25. Abbas MN, Ibrahim SA, Abbas ZN, Ibrahim TA. Eggshells as a sustainable source for acetone production. J King Saud Univ Eng Sci. 2022;34:381–7.
26. Soares MB, Kamogawa MY, Alleoni LRF. Adaptation of calcium acetate methodology to determine the potential acidity of tropical soils. Commun Soil Sci Plan. 2020;51:2701–11.
27. Van Der Sluis P, Schouten A, Spek AL. Structure of a second polymorph of calcium acetate monohydrate. Acta Crystallogr C. 1987;43:1922–4.
28. Klop EA, Schouten A, Van Der Sluis P, Spek AL. Structure of calcium acetate monohydrate, Ca(C$_2$H$_3$O$_2$)$_2$.H$_2$O. Acta Crystallogr C. 1984;40:51–3.

Publisher's Note

Springer Nature remains neutral with regard to jurisdictional claims in published maps and institutional affiliations.